

---

# Sensitivity

## – Local Index to Control Chaoticity or Gradient Globally –

---

Katsunari Shibata   Takuya Ejima   Yuki Tokumaru   Toshitaka Matsuki

katsunarishibata@gmail.com

Oita University

July 21, 2021

### ABSTRACT

In this paper, we propose a fully local index named “sensitivity” for each neuron to control chaoticity or gradient globally in a neural network (NN), and also propose a learning method to adjust it named “sensitivity adjustment learning (SAL)”. The index is the gradient magnitude of its output with respect to its inputs. By adjusting it around 1.0, information transmission in the neuron changes to moderate without shrinking or expanding for both forward and backward computations, and the information transmission through a layer of neurons also moderate when the weights and inputs are random. Therefore, it can be used in a recurrent NN (RNN) to control chaoticity of its global network dynamics, and also can be used to solve the vanishing gradient problem in error back propagation (BP) learning in a deep feedforward NN (DFNN) or an RNN with long-term dependency. We demonstrated that when SAL is applied to an RNN with small random weights, the sum of log-sensitivities is almost equivalent to the maximum Lyapunov exponent until it reaches 0.0 regardless of the network architecture. We also show that SAL works with BP or BPTT to avoid the vanishing gradient problem in a 300-layer DFNN or an RNN solving a problem with 300-step lag between the first input and the output. Compared with the fine manual tuning of the spectral radius of weight matrix before learning, the learning performance was quite better due to the continuous nonlinear learning nature of SAL, which prevented the loss of sensitivity.

**Keywords** sensitivity · sensitivity adjustment learning (SAL) · edge of chaos · recurrent neural network (RNN) · deep feedforward neural network (DFNN) · vanishing gradient problem

## 1 Introduction

Deep learning using a deep feedforward neural network (DFNN) or a recurrent neural network (RNN) has attracted great attention due to its drastic change in the performance especially in recognition of patterns including time-series signals [1, 2, 3, 4]. It has shown the overwhelming power of a massively parallel processing system and acquisition of it through learning. That suggests the way towards the human-like processing, which human designers have struggled to design for a long time, but has not been achieved in the conventional artificial intelligence.

For the development of neural network research hereafter, the processing must be required to be longer in time. Since higher functions such as thinking, language communication cannot be discussed without processing in the time axis, there is no doubt that the significance of temporal processing or dynamics will increase more and more from now on. In the temporal processing, inputs, outputs, and also internal states of a network should not be regarded as a point in space, instead, it should be considered as a line or flow that is formed by a moving point along time.

When it is required to solve a task with long-term dependency, the effective preservation of information in a neural network through time becomes critical. That is deeply related to the chaoticity of the network. If the maximum Lyapunov exponent of the network is negative, much of the information is shrunk and disappears with time. If it is

positive, tiny information is magnified one after another, but rather large information cannot be magnified so much by nonlinearity due to the limited value range of each neuron. Therefore, it is challenging to extract initially large preliminary information from the present internal states after a long time lag. Accordingly, for the effective information preservation through time, dynamics around the edge of chaos is expected to be a right choice.

As for the learning of long-term dependency in an RNN, vanishing/exploding gradient in BPTT (error Back Propagation Through Time) as a gradient-based learning method has been discussed since far before the boom of deep learning[5][6][7]. This problem is originated on a similar basis as the information preservation for a long time lag mentioned earlier. The gradient here is the gradient of some evaluation (can be cost or error) function of final outputs with respect to the weight vector or neuron state vector. By decomposing the gradient by chain rule, we understand the problem comes from the repetition of the information scaling through one time step. A similar discussion can be made for the same problem in deep feedforward NNs (DFNNs). Detailed and related works are described in the next section.

Reservoir computing is often used to learn tasks that need a temporal processing and shows excellent results even though the connection weights among reservoir neurons are not trained. Here, an important parameter is the scale or spectrum radius of weights in the reserver. Echo state property is considered so as that the effect of initial conditions vanish as time passes[8] and if the long-term dependency is learned, the spectral radius should be close to 1.0. In the FORCE learning, the learning performance is good when the network dynamics is around the edge of chaos[9]. We have also shown in reward-modulated Hebbian learning with chaotic exploration using a reservoir network, dynamics around the edge of chaos brings out good learning performance[10][11]. However, the reservoir dynamics cannot be learned, and that is similar to that the hidden representation was given randomly and was not learned in perceptron. Furthermore, there is no idea about how such appropriate random weights are realized in each neuron autonomously without any centralized system. We believe it is highly possible that learning of dynamics is crucial when developing higher functions like "thinking",

When we consider developing a "thinking" machine as an ultimate artificial intelligence system, autonomous transition dynamics in which network state transits autonomously and rationally even without the help of external stimuli must be essential. We expect that similar to the other functions such as "recognition" and "memory", "thinking" emerge within the framework of end-to-end reinforcement learning using an RNN[12]. However, even for externally-driven state transitions, it is not easy for an agent to acquire rational transitions through reinforcement learning using a regular RNN[13] while the acquisition of appropriate memories that do not need transitions is relatively easy[14, 15, 16, 17]

Then, we focused on chaotic dynamics generated in an RNN, and proposed a new reinforcement learning (RL) paradigm [18][19]. In chaotic dynamics, the variation due to a tiny perturbation in a network state is expanded through time. That destabilizes the dynamics and enables autonomous state transition in the RNN although the transition is irregular. In the new proposed RL, the state transition that is based on the internal chaos dynamics is used for exploration instead of the stochastic action selection using random noises. We expect that the irregular dynamics would be changed to be rational by forming attractors on the dynamics through learning. According to the discussion, we set up the hypothesis that 'exploration' grows into 'thinking' through learning. In our study of the new RL, chaoticity of the RNN also should not be either too strong or too weak[20][21]. Adjustment of chaoticity is also critical in this learning paradigm.

The network dynamics is generated as a result of each neuron's processing and the propagated error signals in gradient-based BP (error back propagation) learning including BPTT, represent the influence of small variation in each neuron's state to the final error function. Therefore, we expect that by adjusting the influence of small variation in its inputs to its output in each neuron, the network controls the chaoticity in RNN dynamics and the propagation of the error signals simultaneously. In this paper, we define the magnitude of the gradient of its output with respect to its input vector as "sensitivity" in each neuron. We also introduce a learning method to adjust the sensitivity according to a gradient-based hill-climbing method, and call it "sensitivity adjustment learning (SAL)". Then we show that an RNN generates chaotic dynamics through SAL, and the relation between the sensitivities as a local index and the maximum Lyapunov exponent as a global index during learning is observed at first. We also show supervised learning results of a simple problem with 300 step lag between the first input and final output timings in an RNN using both BPTT and SAL, and the learning process is analyzed. Finally, we apply SAL to DFNNs with BP and show a 300 layer DFNN can learn a simple problem with noise addition and observe the processing.

## 2 Related Works

In order to avoid the vanishing/exploding gradient in gradient-based error back propagation (BP) including BPTT (Back Propagation Through Time), several techniques have been already proposed. They can be roughly divided into two categories.

In the first category, which is mainly focus on RNNs whose feedback weight matrix is square, the spectral radius of the Jacobian matrix between the inputs and outputs of a layer or group of neurons is directly set to be around 1.0. The simplest way is to set the Jacobian matrix close to the identity matrix. In this case, the output vector is identical to the input vector. Therefore, a small variation in each of the neuron state does not change through the forward processing. The error signal in each neuron also does not change through the backward processing.

In LSTM[22], which is a quite popular RNN, special units namely LSTM cells are employed, and if the forgetting gate is fully open, the cell state does not change and each diagonal element of the Jacobian matrix is close to 1.0 when we only focus on the signal flow through time at the cell. GRU[23] has a simpler but similar structure to LSTM. We have adopted a simpler method in which all the feedback connection weights are initially set to 0.0 or small random values except for the self feedback connection weights, which are set to the reciprocal of the maximum derivative value of the activation function. Concretely, the weight value is 4.0 for the sigmoid function and 1.0 for the hyperbolic tangent. In this case, the Jacobian matrix is close to the identity matrix when the activations are small enough in the activation function’s linear region. It works well in learning of memory-required tasks[14, 15, 16, 17], which needs to form fixed-point attractors or static associative memory. In FNNs, shortcut connections through one or more layers as in a ResNet[24], which is widely used mainly to convolutional NNs (CNNs), also realize its Jacobian matrix to be close to the identity matrix if the other connection weight values are small.

However, the transformation represented by the identity matrix is equivalent to no processing being done. Therefore, it is suitable to keep some information without any change, but it is difficult to expect a complicated conversion of input signals or internal dynamic state transition like “thinking”. Actually, in our work[13], simple state transitions could be realized through learning in this approach, but despite the simple transitions, learning was so difficult that careful design of task shaping is necessary.

In the second category, mean and variance of neuron activations are normalized, usually to zero mean and unit variance. Batch normalization[25], layer normalization[26], weight normalization[27], self-normalizing neural network[28] can be categorized in a broad meaning. In the self-normalizing neural network, by setting the weight matrix and activation function appropriately, the activations close to zero mean and unit variance converge towards zero mean and unit variance. Furthermore, the variance of neuron activations is bounded and the network does not suffer from a vanishing gradient. In the weight normalization process, the weight vectors are initialized depending on the given data so that the mean and variance of neuron activations are normalized.

Different from the approaches mentioned above, Moderatism aims to acquire necessary processing by keeping the variation of both inputs and output in each neuron moderate[29]. In this paper, we focus on the sensitivity that represents magnification or contraction of a small variation in each neuron’s processing, and by controlling it in each neuron, the global dynamics of the network is controlled. We show that adjusting each neuron’s sensitivity enables learning for DFNNs or RNNs with a long time-lag problem.

On the other hand, from the viewpoint of chaos control, previous studies have mainly focused on stabilize a system with chaotic dynamics[30][31], and have not positively utilized the chaos or edge of chaos dynamics. From the information storage or processing perspective, the importance of “edge of chaos” has been highlighted by several studies[32][33][34]. Moreover, from the biological viewpoint, the relation between known input stimuli and attractors in the brain dynamics was investigated and the role of the chaotic dynamics for new input stimuli was addressed[35][36]. An associative memory model based on the study using a chaotic neural network was also proposed[37]. However, it’s not easy to find a method that can generate and control chaos dynamics by learning in an RNN. Consequently, dynamics around the edge of chaos produced in an RNN with fixed weights has been utilized as a reservoir as mentioned above. In this paper, we also propose to generate and control the network chaoticity by adjusting local sensitivity in each neuron to utilize chaos or edge of chaos dynamics positively.

### 3 Sensitivity and Sensitivity Adjustment Learning (SAL)

#### 3.1 Definition of Sensitivity

Figure 1 shows a general static-type neuron model with  $m$  inputs. Its internal state  $u$  is derived as the inner product of the input vector  $\mathbf{x} = (x_1, \dots, x_m)^T$  and connection weight vector  $\mathbf{w} = (w_1, \dots, w_m)^T$  as

$$u = \mathbf{w} \cdot \mathbf{x}, \quad (1)$$

and the output  $o$  is derived as

$$o = f(U) = f(u + \theta), \quad (2)$$

where  $U = u + \theta$ ,  $\theta$  is the bias, and  $f()$  is an activation function that can be hyperbolic tangent or sigmoid function. Sensitivity proposed here is a local index for each neuron to show how a neuron is sensitive to a small change in its

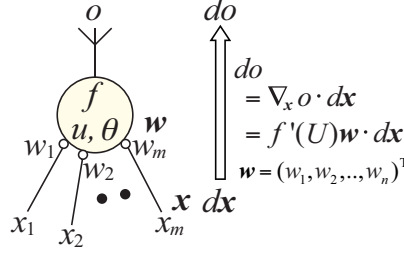


Figure 1: A neuron model and change of the small deviation between its input vector and output.

inputs. It is defined as the Euclidean norm of the output gradient with respect to the input vector  $\mathbf{x}$  as

$$s(\mathbf{x}) = |\nabla_{\mathbf{x}} o| = f'(U) |\mathbf{w}| \quad (3)$$

if the activation function  $f$  is a monotonically increasing function. If the vector elements are used, it is rewritten as

$$s(\mathbf{x}) = \sqrt{\sum_i^m \left( \frac{\partial o}{\partial x_i} \right)^2} = f'(U) \sqrt{\sum_i^m w_i^2}. \quad (4)$$

### 3.2 Sensitivity in the forward computation

In the forward computation in the neuron, as shown in Fig. 1, an infinitesimal change in the inputs  $d\mathbf{x}$  produces the infinitesimal change in the output  $do$  as

$$do = \nabla_{\mathbf{x}} o \cdot d\mathbf{x} = |\nabla_{\mathbf{x}} o| |d\mathbf{x}| \cos \phi = s(\mathbf{x}) |d\mathbf{x}| \cos \phi. \quad (5)$$

where  $\cos \phi$  is the direction cosine between the input change vector  $d\mathbf{x}$  and the weight vector  $\mathbf{w}$  whose direction is the same as the gradient vector.

Here, the distribution of each element  $dx_i$  of the vector  $d\mathbf{x}$  is assumed to be i.i.d. (independent and identically distributed) with mean 0. From symmetry, the mean square of the magnitude of the vector  $d\mathbf{x}$  is  $m$  times of the variance of each element as

$$E [ |d\mathbf{x}|^2 ] = \sum_i^m V [dx_i] = m V [dx_i]. \quad (6)$$

On the other hand, if the weight vector  $\mathbf{w}$  is a random vector whose elements are chosen from i.i.d. distribution with mean 0, the variance of the direction cosine is

$$V [\cos \phi] = E [\cos^2 \phi] = \frac{1}{m} \quad (7)$$

also from symmetry. Therefore, from Eq. (5), the variance of the output change  $do$  can be written using the variance of one input change  $dx_i$  and its sensitivity  $s$  as

$$V [do] = \frac{s^2(\mathbf{x})}{m} E [ |d\mathbf{x}|^2 ] = s^2(\mathbf{x}) V [dx_i]. \quad (8)$$

If the sensitivity  $s(\mathbf{x}) = |\nabla_{\mathbf{x}} o|$  is 1.0, then the output change in Eq. (5) can be written as

$$do = |d\mathbf{x}| \cos \phi, \quad (9)$$

and that is the projection of  $m$ -dimensional infinitesimal vector  $d\mathbf{x}$  onto the direction of the weight vector  $\mathbf{w}$  as shown in Fig. 2. In this case, Eq. (8) can be modified as follows:

$$V [do] = V [dx_i]. \quad (10)$$

This is significant because the neuron maintains the variance equivalent for one input signal as its own output variance without being shrunk or expanded not depending on the number of connections  $m$ .

For example, suppose  $d\mathbf{x}$  is an  $m$ -dimensional standard normal random vector after the multiplication of an infinitesimal constant  $\epsilon$  as  $d\mathbf{x} \sim \mathcal{N}(0, \epsilon^2 I_m)$  where  $I_m$  is the  $m$ -dimensional unit matrix. That means that the distribution of the vector is a gaussian point cloud. The distribution of the vector direction is uniform, and that is the same as the case

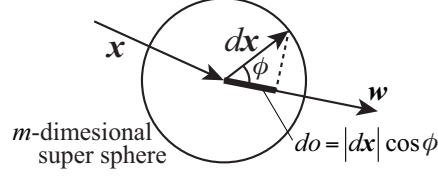


Figure 2: When the sensitivity  $s$  is 1.0, the output change  $do$  is the projection of the infinitesimal input vector change  $dx$  on to the weight vector  $w$ . Therefore, when  $dx$  is distributed uniformly on a super sphere, the expectation of  $|do|$  is equivalent to that of one of the  $m$  input signals.

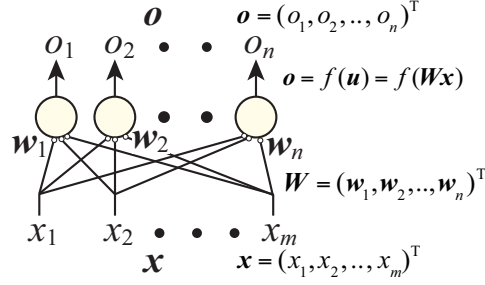


Figure 3: Forward (output) computation through a layer of neurons.

of the  $m$ -dimensional super sphere surface as presented in Fig. 2. The change in the output  $do$  is the projection of  $dx$  into one direction in the  $m$ -dimensional space, and so  $do \sim \mathcal{N}(0, \epsilon^2)$  not depending on the number of inputs  $m$ .

Next, the case of a group or layer of  $n$  neurons as can be seen in Fig. 3 is considered, and its output vector is indicated as  $\mathbf{o} = (o_1, \dots, o_n)^T$ . The infinitesimal output change  $d\mathbf{o}$  can be represented using the small input change  $d\mathbf{x}$  as

$$d\mathbf{o} = J(\mathbf{x})d\mathbf{x} \quad (11)$$

using Jacobian matrix

$$J(\mathbf{x}) = \begin{pmatrix} \frac{\partial o_1}{\partial x_1} & \dots & \frac{\partial o_1}{\partial x_m} \\ \vdots & \ddots & \vdots \\ \frac{\partial o_n}{\partial x_1} & \dots & \frac{\partial o_n}{\partial x_m} \end{pmatrix} = \begin{pmatrix} (\nabla_{\mathbf{x}} o_1)^T \\ \vdots \\ (\nabla_{\mathbf{x}} o_n)^T \end{pmatrix}. \quad (12)$$

Eq. (11) can be rewritten using sensitivities of the neurons as

$$d\mathbf{o} = \begin{pmatrix} \nabla_{\mathbf{x}} o_1 \cdot d\mathbf{x} \\ \vdots \\ \nabla_{\mathbf{x}} o_n \cdot d\mathbf{x} \end{pmatrix} = \begin{pmatrix} s_1(\mathbf{x})|d\mathbf{x}| \cos \phi_1 \\ \vdots \\ s_n(\mathbf{x})|d\mathbf{x}| \cos \phi_n \end{pmatrix}, \quad (13)$$

The distribution of each element of the infinitesimal change in the input vector  $dx_i$  is assumed to be i.i.d. with mean 0 as above. If the weight matrix  $\mathbf{W}$  is an  $n \times m$  random matrix and the number of input  $m$  is large enough, the distribution of each element of the infinitesimal change of the output vector  $do_j$  is also i.i.d. with mean 0. The mean square of the magnitude of the vector  $d\mathbf{o}$  is  $n$  times of the variance of one output change  $do_j$  as

$$E[|d\mathbf{o}|^2] = \sum_j^n V[do_j] = nV[do_j]. \quad (14)$$

From Eq. (8),

$$\frac{1}{n}E[|d\mathbf{o}|^2] = \frac{\langle s^2(\mathbf{x}) \rangle}{m}E[|d\mathbf{x}|^2] \quad (15)$$

where  $\langle s^2(\mathbf{x}) \rangle$  is the average of  $s^2(\mathbf{x})$  over the  $n$  neurons. If  $\langle s^2(\mathbf{x}) \rangle = 1.0$  or the sensitivity of each neuron is 1.0, then

$$\frac{\text{RMS}[|d\mathbf{o}|]}{\sqrt{n}} = \frac{\text{RMS}[|d\mathbf{x}|]}{\sqrt{m}} \quad (16)$$

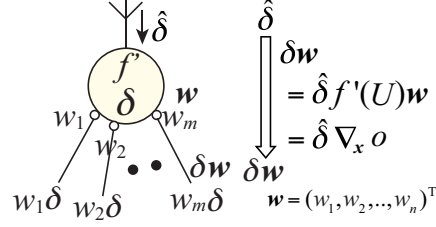


Figure 4: Backward (error signal) computation in a neuron.

where RMS means root mean square. If the numbers of inputs and outputs are the same, then

$$\text{RMS} [|\mathbf{d}\mathbf{o}|] = \text{RMS} [|\mathbf{d}\mathbf{x}|] \quad (17)$$

From the above discussion, if each neuron's sensitivity is 1.0, the distribution of the small change in each neuron is maintained not depending on the number of neurons or number of inputs. Accordingly, a small change in an input signal of the network can be expected to reach the final network output even though (1) the number of layers is large, (2) the number of neurons in each layer is varied and/or (3) the connection between layers is sparse. The same discussion can also be applied to an RNN. The distribution of small output change is maintained through time regardless of the structure of the RNN, such as sparse or full connections, flat (non-layered) or layered. Accordingly, if the sensitivities for all the neurons are around 1.0 and stable, the maximum Lyapunov exponent as the logarithm of time development of small change is expected to be around 0.0.

### 3.3 Sensitivity in the backward computation

As mentioned earlier, when a small change in network inputs reaches the network outputs, the error signals for learning propagating backward through the network based on gradient descent, such as BP or BPTT, reaches the input layer from the output layer in the backward computation for learning. A neuron receives an error signal for its output  $\hat{\delta} = \partial E / \partial o$ . Error signal  $\delta$  for its internal state  $u$  is derived by multiplying the derivative of its activation function to  $\hat{\delta}$  as

$$\delta = \frac{\partial E}{\partial u} = \frac{\partial E}{\partial o} \frac{do}{du} = \hat{\delta} f'(U). \quad (18)$$

As depicted in Fig. 4, the error signal is propagated after being weighted by the weight vector  $\mathbf{w}$  before propagating to the one-level lower layer neurons. Then the propagated error signal vector  $\delta \mathbf{w}$  can be written as

$$\delta \mathbf{w} = \hat{\delta} f'(U) \mathbf{w} = \hat{\delta} \nabla_{\mathbf{x}} o. \quad (19)$$

Therefore, the magnitude of it can be expressed as

$$|\delta \mathbf{w}| = \left| \hat{\delta} \nabla_{\mathbf{x}} o \right| = \left| \hat{\delta} \right| \left| \nabla_{\mathbf{x}} o \right| = s(\mathbf{x}) \left| \hat{\delta} \right|, \quad (20)$$

and if the sensitivity  $s(\mathbf{x}) = \left| \nabla_{\mathbf{x}} o \right|$  is 1.0, then

$$|\delta \mathbf{w}| = \left| \hat{\delta} \right|, \quad (21)$$

and the error signal is propagated efficiently without being shrunk or expanded through the neuron.

From the view of group or layer of neurons, the relation between the error signal before and after the layer  $\hat{\delta}_{before}$ ,  $\hat{\delta}_{after}$  can be written as

$$\hat{\delta}_{after} = \mathbf{W}^T \left( f'(U) \otimes \hat{\delta}_{before} \right) \quad (22)$$

Jacobian matrix as presented in Eq. (12) can be modified as

$$\begin{aligned} J(\mathbf{x}) &= \begin{pmatrix} f'(U_1)w_{11} & \cdots & f'(U_1)w_{1m} \\ \vdots & \ddots & \vdots \\ f'(U_n)w_{n1} & \cdots & f'(U_n)w_{nm} \end{pmatrix} \\ &= (f'(U_1)\mathbf{w}_1, \dots, f'(U_n)\mathbf{w}_n)^T. \end{aligned} \quad (23)$$

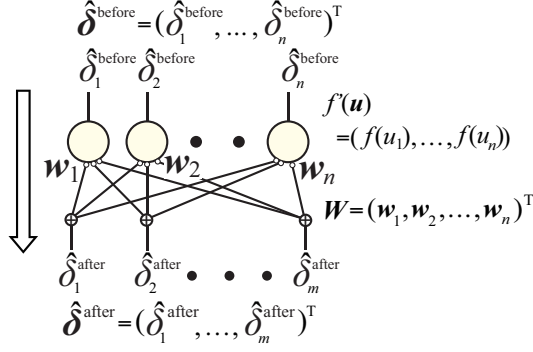


Figure 5: Backward computation through a layer of neurons.

So, Eq. (22) is changed to

$$\hat{\delta}_{\text{after}} = J^T(\mathbf{x})\hat{\delta}_{\text{before}} \quad (24)$$

Accordingly, though the Jacobian matrix is transposed, the same discussion as the relation between  $|do|$  and  $|dx|$  in the forward computation can be made. The expectations of the mean squared error signal before and after the layer can be found as

$$\frac{1}{m}E \left[ |\hat{\delta}_{\text{after}}|^2 \right] = \frac{\bar{s}^2}{n}E \left[ |\hat{\delta}_{\text{before}}|^2 \right] \quad (25)$$

If the sensitivity of each neuron is 1.0,

$$\frac{\text{RMS} \left[ |\hat{\delta}_{\text{after}}| \right]}{\sqrt{m}} = \frac{\text{RMS} \left[ |\hat{\delta}_{\text{before}}| \right]}{\sqrt{n}}, \quad (26)$$

and the error signals in backward computation do not either disappear or explode. If the numbers of inputs and outputs are the same, RMS remains unchanged before and after the layer as stated below:

$$\text{RMS} \left[ |\hat{\delta}_{\text{after}}| \right] = \text{RMS} \left[ |\hat{\delta}_{\text{before}}| \right]. \quad (27)$$

Therefore, if all network neurons sensitivities can be controlled around 1.0, it is expected that the error signals propagate backward without being shrunk or expanded.

### 3.4 Learning Method

In sensitivity adjustment learning (SAL), which is also proposed in this paper, each neuron has a small weight vector initially, and updates them to increase its sensitivity by hill climbing that is the steepest ascent according to

$$\Delta \mathbf{w} = \eta_{SAL} \nabla_{\mathbf{w}} s(\mathbf{x}) = \eta_{SAL} \nabla_{\mathbf{w}} |\nabla_{\mathbf{x}} o| \quad (28)$$

where  $\eta_{SAL}$  is the learning rate for SAL. From Eq. (3),

$$\begin{aligned} \nabla_{\mathbf{w}} |\nabla_{\mathbf{x}} o| &= \nabla_{\mathbf{w}} \{f'(U) |\mathbf{w}|\} \\ &= f'(U) \nabla_{\mathbf{w}} |\mathbf{w}| + |\mathbf{w}| \nabla_{\mathbf{w}} f'(U) \\ &= f'(U) \frac{\mathbf{w}}{|\mathbf{w}|} + |\mathbf{w}| \nabla_{\mathbf{w}} f'(U) \end{aligned} \quad (29)$$

Then the update rule can be written as

$$\Delta \mathbf{w} = \eta_{SAL} \left( f'(U) \frac{\mathbf{w}}{|\mathbf{w}|} + |\mathbf{w}| \nabla_{\mathbf{w}} f'(U) \right). \quad (30)$$

In the following simulations, we use tanh as activation function  $f(\cdot)$  for all the neurons. In this case,

$$f'(U) = \frac{1}{\cosh^2(U)} = 1 - o^2 \quad (31)$$

and so

$$\begin{aligned}\nabla_{\mathbf{w}}f'(U) &= \nabla_{\mathbf{w}}(1 - o^2) \\ &= -2of'(U)\nabla_{\mathbf{w}}U \\ &= -2o(1 - o^2)\mathbf{x}.\end{aligned}\quad (32)$$

Then the update rule is as

$$\Delta\mathbf{w} = \eta_{SAL}(1 - o^2) \left( \frac{\mathbf{w}}{|\mathbf{w}|} - 2o|\mathbf{w}|\mathbf{x} \right). \quad (33)$$

In this equation, the term  $\eta_{SAL}(1 - o^2)\mathbf{w}/|\mathbf{w}|$  is originated from the first term of the right-hand side of Eq. (29). This means the sensitivity is increased directly by making the corresponding absolute weight value larger.  $\mathbf{w}/|\mathbf{w}|$  is the unit vector whose direction is the same as  $\mathbf{w}$ . Accordingly, if the neuron output is around the linear region, in which the output is around 0.0, the weight vector  $\mathbf{w}$  becomes larger at a constant rate of  $\eta_{SAL}$  while keeping its direction. The second term  $-2\eta_{SAL}(1 - o^2)o|\mathbf{w}|\mathbf{x}$  is originated from the second term of the right-hand side of Eq. (29). This means the sensitivity is increased indirectly by making the internal state's magnitude smaller for large  $f'(U)$ . This term works only after the neuron is out of the linear region of the activation function.

Different from the case of weight, bias  $\theta$  cannot increase the sensitivity directly, but can increase it indirectly by updating the bias so that the value  $U$  becomes closer to 0.0. Accordingly, the update rule for the bias is indicated as

$$\Delta\theta = \eta_{SAL}|\mathbf{w}|\frac{\partial f'(U)}{\partial\theta}. \quad (34)$$

Furthermore, assuming the activation function is tanh, it can be rewritten as

$$\Delta\theta = -2\eta_{SAL}o(1 - o^2)|\mathbf{w}|. \quad (35)$$

When supervised learning is performed together with SAL learning, error back propagation (BP) learning based on stochastic gradient descent (SGD) is used such as

$$\Delta\mathbf{w} = -\eta_{BP}\nabla_{\mathbf{w}}E \quad (36)$$

where  $E$  is the squared error when a training signal vector  $\mathbf{d}$  is given and is expressed as

$$E = \frac{1}{2}(\mathbf{d} - \mathbf{o}^{out})^2 \quad (37)$$

where  $\mathbf{o}^{out}$  is the output vector in the output layer. In this paper, assuming simple on-line learning, no batch learning is done, and the network is trained for each presented pattern one by one.

Furthermore, an additional technique to avoid the exploding gradient problem is introduced here. The function tanh is equivalent to the identity function when the input is around 0.0, but the output is saturated when the absolute value of the input is large. Then, when the error signal is computed, the function tanh is applied after multiplication of the derivative  $f'()$ . Instead of applying Eq. (18), the error signal is computed as

$$\delta = \tanh(\hat{\delta}f'(U)), \quad (38)$$

and the weight vector is updated as

$$\Delta\mathbf{w} = \eta_{BP}\delta\mathbf{x}. \quad (39)$$

In this paper, when BP or BPTT is applied with SAL, the weights are updated by SAL just after the forward computation at each timing in each neuron when the moving average of sensitivity  $\bar{s}$  for the neuron is less than 1.0, and once all the forward computations for the presented pattern are completed, BP or BPTT is applied in the backward computation. The flowchart for the case of learning of an RNN with BPTT, as an example, is shown in Fig. 6. However, when its output fluctuates largely, the sensitivity value in Eq. (3) fluctuates significantly because the  $f'(U) = 1 - o^2$  varies between 0.0 and 1.0 depending on the output. Therefore, the moving average of sensitivity  $\bar{s}$  in each neuron is introduced as

$$\bar{s}_n \leftarrow \beta\bar{s}_{n-1} + (1 - \beta)s_n \quad (40)$$

where  $\beta$  is a decay rate, and SAL is applied only when  $\bar{s}$  is less than 1.0 when using with BP or BPTT.



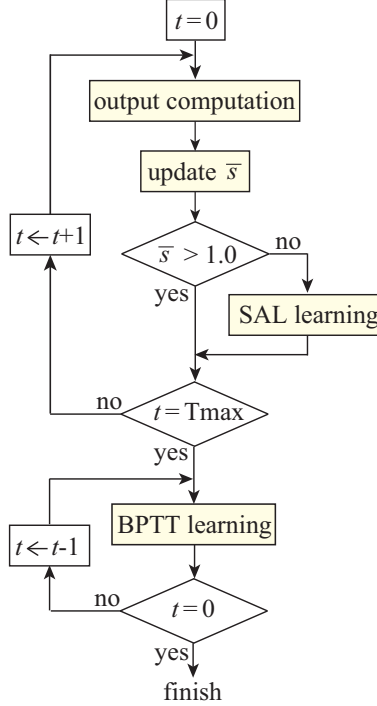


Figure 6: Flow chart for the parallel learning of SAL and BPTT. SAL is applied only when the moving average of the sensitivity is less than 1.0. This conditional branch and SAL itself are performed individually in each neuron.

## 4 Simulations

The following simulations are roughly divided into two parts. In the first part as described in subsection 4.1, only sensitivity adjustment learning (SAL) is applied to recurrent neural networks (RNNs). Generation and control of chaotic dynamics are examined and the relation between sensitivities and maximum Lyapunov exponent is focused on. In the second part described in subsection 4.2, both SAL and supervised learning using BP or BPTT are applied, and then the performance is observed, and the learning process is analyzed. In all the simulations, hyperbolic tangent tanh is used as the activation function of each neuron.

### 4.1 Generation and Control of Chaos

At first, we show the generation of chaos dynamics and adjustment of chaoticity by sensitivity adjustment learning (SAL) using RNNs for various network architectures.

Before entering the simulation result, it is explained how the maximum Lyapunov exponent is approximated here. At every 100 steps ( $t = 0, 100, 200, \dots$ ), two internal states,  $\mathbf{u}_0^{(1)} = \mathbf{u}_t$  and  $\mathbf{u}_0^{(2)} = \mathbf{u}_t + \mathbf{rnd}$  where  $\mathbf{rnd}$  is a small random vector whose size is  $10^{-3}$ , are prepared. The two states are updated separately without updating the weights. At each

Table 1: Parameters for chaos generation by SAL using a flat RNN

number of neurons	100 or 30
connection rate (%)	100 or 30
initial connection weights	uniformly random [-0.01, 0.01]
learning rate $\eta_{SAL}$ in Eq. (33)	0.00002
decay rate $\beta$ in Eq. (40)	0.99
perturbation (interval, size)	(1000, 0.001)

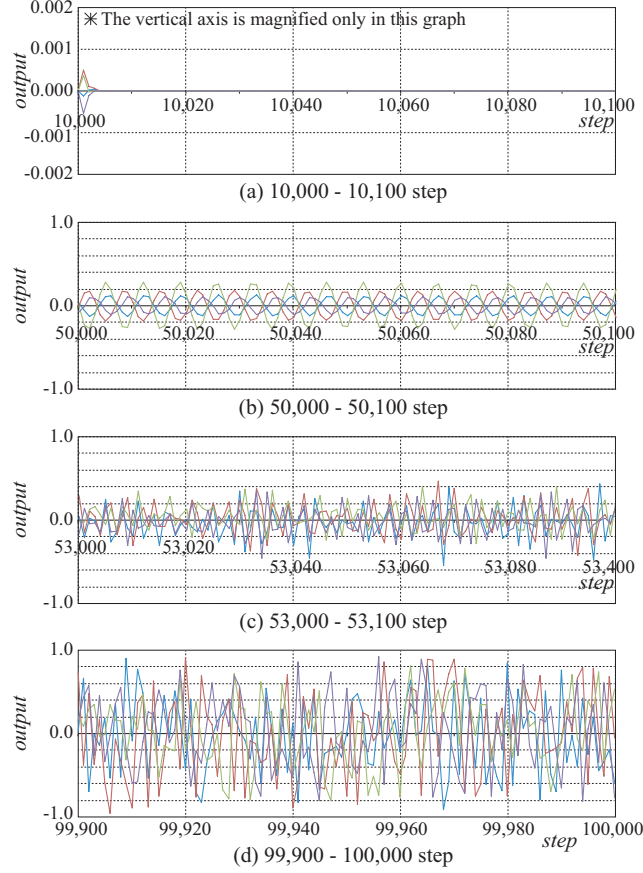


Figure 7: Change of 4 sample time-series of outputs as learning progresses when SAL is applied to a flat RNN

step  $\tau$ , the distance ratio between before and after one step update is calculated as

$$l_{\tau} = \ln \left( \frac{\mathbf{u}_{\tau}^{(2)} - \mathbf{u}_{\tau}^{(1)}}{10^{-3}} \right). \quad (41)$$

After that, the distance is normalized to  $10^{-3}$  as

$$\mathbf{u}_{\tau}^{(2)} \leftarrow \frac{10^{-3}}{|\mathbf{u}_{\tau}^{(2)} - \mathbf{u}_{\tau}^{(1)}|} \left( \mathbf{u}_{\tau}^{(2)} - \mathbf{u}_{\tau}^{(1)} \right) + \mathbf{u}_{\tau}^{(1)}. \quad (42)$$

Finally, the maximum Lyapunov exponent is computed using the last 200 steps in a total of 300 steps of the forward computation as

$$\lambda = \frac{1}{200} \sum_{\tau=101}^{300} l_{\tau}. \quad (43)$$

When the network has two layers, that is computed at the 1st layer.

#### 4.1.1 Case of Flat RNN

Firstly, we investigate using a flat RNN in which no layer structure is introduced and the neurons are mutually connected. The parameters are presented in Table 1. The initial connection weights are small uniform random numbers, and no bias is used here. The learning rate is very small to see the dynamics for each stage during learning. A small random perturbation is added to the internal state vector  $\mathbf{u}$  at every 1000 steps from the 1st step as a trigger of activations.

In the first simulation, using an RNN with fully connected 100 neurons, learning process is shown in detail. Each of the four figures in Fig. 7 shows the output changes of 4 sample neurons for one of the 4 stages during learning. In

an early phase, although small perturbation is added, the output is decayed soon as shown in Fig. 7 (a). Around the 50,000th step, the outputs change almost periodically as can be seen in Fig. 7 (b), and around the 53,000th step, the outputs change irregularly as shown in Fig. 7 (c). Around the 100,000th step, the outputs still change irregularly, but the value range is larger as shown in Fig. 7 (d).

Figure 8 shows how learning progresses from various aspects. Figure 8 (A) provides the maximum and mean absolute value of the output over all the neurons. Before around the 45,000th step indicated by the thick vertical broken line, all the outputs were almost 0.0 though small perturbations were added. Around the 45,000th step, the outputs became larger suddenly. After that, they became gradually larger with some fluctuations, and finally they varied in most of the value range as can be seen in Fig. 7(d). Figure 8(B) shows how some of the weights change during learning. Before around the 45,000th step when the outputs of all the neurons are in the linear region, the absolute value of each weight grows constantly into large values, which is consistent with Eq. (33). After that, the weight value still tends to increase, but sometimes it decreases and sometimes the magnitude relation between two weights is switched.

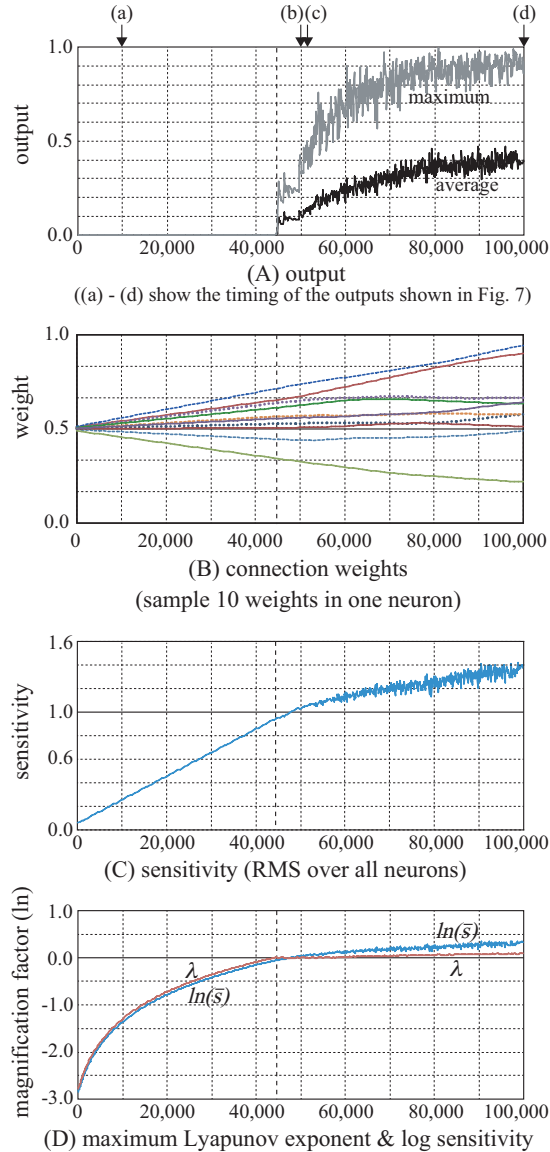


Figure 8: Learning process when SAL is applied to a flat RNN. (A) The maximum and average of 100 outputs. (B) Connection weight change. (C) RMS of sensitivities over all the neurons, (D) maximum Lyapunov exponent and log sensitivity (logarithm of the (C) value). All the data are plotted at every 100 steps. The thick vertical broken line shows the boundary whether the outputs decays to 0.0 or not.

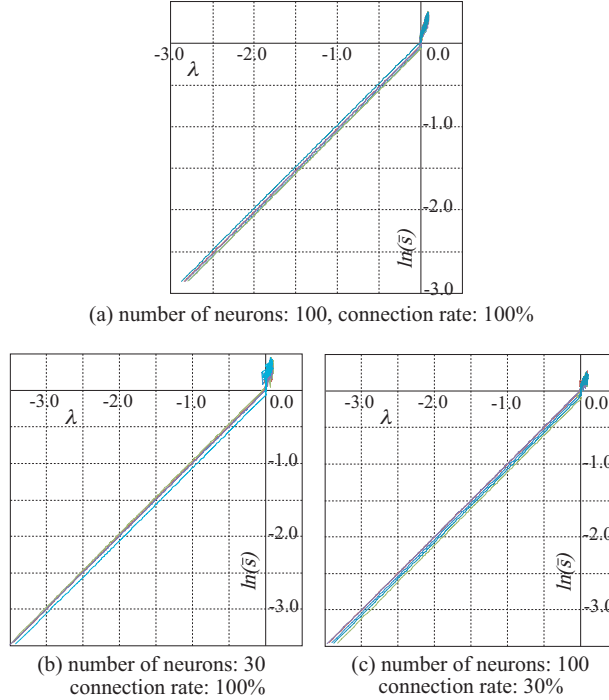


Figure 9: Relation between the maximum Lyapunov exponent and log-sensitivity during SAL for 5 cases varying the number of neurons or connection ratio.

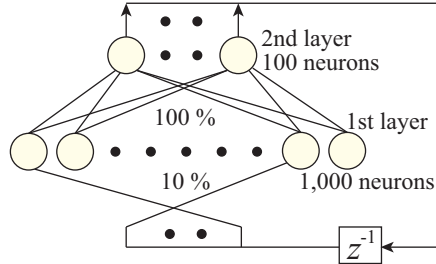


Figure 10: Two-layer RNN. SAL is applied to all the neurons in the network.

Figure 8(C) presents the change of RMS of the sensitivities over all the neurons during learning. It increases almost linearly until it reaches to 1.0 right after the neurons take non-zero values. Next, the increase rate becomes smaller and the value is fluctuating. In order to compare with the maximum Lyapunov exponent, which shows the chaoticity of the network dynamics, the RMS sensitivity is plotted on the log-scale in Fig. 8(D). The value is called log-sensitivity here. The maximum Lyapunov exponent  $\lambda$  is also plotted on the same graph. We can see that before around the 45,000th step, they are almost the same. Afterward, the slope for  $\lambda$  becomes smaller than that for log-sensitivity, but  $\lambda$  is still increasing. Then we plot the relationship between the maximum Lyapunov exponent  $\lambda$  and log-sensitivity  $\ln(\bar{s})$  by taking them as  $x$  and  $y$  axes respectively shown in Fig. 9(a). 5 lines are plotted for 5 cases of different initial connection weights decided randomly. All of the 5 cases are almost similar, and when the log-sensitivity reaches to 0.0, the maximum Lyapunov exponent is almost 0.0.

Then we change the number of neurons or connection rate, and examine whether the same relationship can be seen between the maximum Lyapunov exponent and the log-sensitivity. Fig. 9(b) shows the results when the number of neurons is decreased to 30. When the connection rate is decreased to 30%, the results can be seen in Fig. 9(c). We can see that the maximum Lyapunov exponent is almost identical to the log-sensitivity as well as the case of 100 neuron fully connected network. Only the difference is the starting value is almost -3.5 in (b) and (c), but originally it is around -2.8. Those are almost the same as the expected value  $\ln(\text{RMS}[\|\mathbf{w}\|])$  derived from Eq. (3). Since the initial weight values are decided as a uniform random number from -0.01 to 0.01,  $\text{Var}[w_i] = 10^{-4}/3$ .  $m$  is 100 in (a), 30 in (b) and (c) and  $f'(U) \approx 1.0$ .

Table 2: Parameters for chaos generation by SAL using a 2-layer RNN

number of neurons	1000 (1st) 100 (2nd)
connection rate (%)	100 (2nd $\leftarrow$ 1st) 10 (1st $\leftarrow$ 2nd)
initial connection weights	uniformly random [-0.03, 0.03]
learning rate $\eta_{SAL}$ in Eq. (33)	0.00002
decay rate $\beta$ in Eq. (40)	0.99
perturbation (interval, size)	(1000, 0.001)

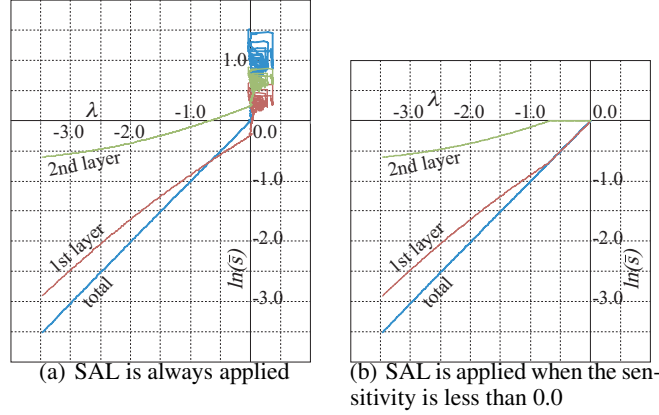


Figure 11: Relation between the maximum Lyapunov exponent and log-sensitivity during SAL with 1.0 maximum sensitivity (1000-100neurons, 10%-100% connection rate)

#### 4.1.2 Case of Two-Layer RNN

We examine the relationship between the maximum Lyapunov exponent and log-sensitivity in multi-layer recurrent neural network (RNN). Here, we employ two-layer RNN as shown in Fig. 10. The first layer has 1000 neurons and the second layer has 100 neurons. The connection rate from the first layer to the second layer is 100%. In contrast, the feedback connection from the second layer to the first layer is 10%. The expected number of connections is 10 for the first layer neurons, while that is 1000 for the second layer neurons. The parameters are summarized in Table 2.

Figure 11(a) shows the relationship between each layer's log-sensitivity and the maximum Lyapunov exponent. Here we also employ total log-sensitivity that is the sum of the log-sensitivities of both layers. The sensitivity value is mainly different between the two layers because the number of connections is largely different. As learning progresses, the log-sensitivities become large, and in the second layer, it became larger than 0.0 though the maximum Lyapunov exponent is still negative. However, we can see that the total log-sensitivity is almost the same as the maximum Lyapunov exponent, and when the total log-sensitivity is 0.0, the maximum Lyapunov exponent is around 0.0

Then to adjust the network dynamics to be around the edge of chaos, SAL was stopped in each neuron when the moving average of its sensitivity as in Eq. (40) reached 1.0. Figure 11(b) displays the results. We can see that the second layer's log-sensitivity did not become larger than 0.0, and finally the network dynamics reached and maintained around the edge of chaos that is the dynamical state around the maximum Lyapunov Exponent  $\lambda = 0.0$ .

## 4.2 Solving vanishing gradient problem

Next, it is focused on how the sensitivity adjustment learning (SAL) works to avoid vanishing gradient problem in the backward computation for gradient-based learning. In this learning, SAL is applied in each neuron only when the sensitivity is below 1.0 following the flowchart as presented in Fig. 6.

In the following, we show two cases of supervised learning. The first one is a recurrent neural network (RNN) solving a problem with long-term dependency, and the network is trained by BPTT (error Back Propagation Through Learning). The second one is a deep feedforward network (DFNN) trained by BP (error Back Propagation). In each case, in order

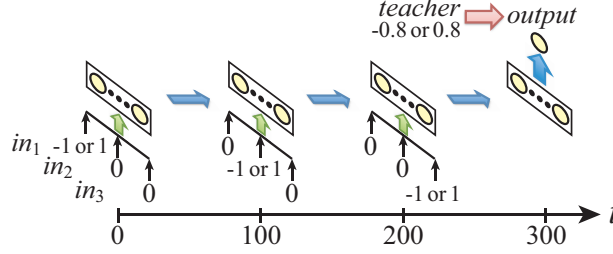


Figure 12: Sequential 3-bit parity problem with 3 inputs at intervals of 100 steps.

Table 3: Parameters for supervised learning of RNNs using SAL and BPTT.

number of hidden neurons		20
initial connection weights (uniformly random)	input $\rightarrow$ hidden	0.0
	hidden $\rightarrow$ output	$[-0.3, 0.3]$
	hidden $\rightarrow$ hidden	$[-0.1, 0.1]$
learning rate $\eta_{SAL}$ in Eq. (33)		0.0002
learning rate $\eta_{BP}$ in Eq. (36)	input $\rightarrow$ hidden	0.4
	hidden $\rightarrow$ output	0.1
	hidden $\rightarrow$ hidden	0.00004
decay rate $\beta$ in Eq. (40)		0.999

to see how SAL works in the gradient-based learning, we choose a simple learning problem and stochastic gradient descent (SGD).

#### 4.2.1 Case of RNN with a Long Time-Lag Problem

Here, in order to see how the SAL affects the gradient-based supervised learning, we employ a simple 3-layer Elman-type RNN whose hidden outputs are fed back to themselves at the next time step. As a simple learning problem, sequential 3-bit parity problem with 300 step time-lag as shown in Fig. 12 is given. In the problem, 3 inputs are given sequentially at every 100 steps and the training signal is given 300 steps after the timing of the first input.

Table 3 presents the parameters used here. The propagated error signals and sensitivities during learning are observed as well as the learning performance. 100 simulations are performed with different random initial connection weights. Here, sensitivities are computed at every timing except for  $t = 0$  in each hidden neuron and only the feedback weight vector  $\mathbf{w}_{FB}$  is used to compute them according to Eq. (3). Successful learning is defined as the case when the absolute value of the error is less than 0.01 for all the 8 patterns within 1000 epochs.

Fig. 13 (a) shows the success ratio when both SAL and BPTT are applied. We call it 'original' for the following comparison. There is only one failure in 100 runs, but even in the failure case, the network could learn it in 3000 epochs. Fig. 14 (A) shows the learning process of a standard run whose learning is 46th fastest in 100 runs. (The initial weights also will be used later as a sample of failures in (c)) Figures (1) and (2) depict the learning curve and output change for each of 8 patterns during learning. Note that in the 0th epoch that includes 8 pattern presentations, no learning was applied to show the outputs and error signals before learning. We can see that the error decreased gradually except when it temporarily increased around the 30th epoch.

Figure (3) shows how the RMS of the error signal  $\delta$  changed in BPTT in the hidden layer during learning. Before learning, the error signal at the 300th step, which is the output timing, is around  $10^{-1}$ , but for each input timing (200th, 100th, 0th step), it was far smaller than  $10^{-30}$ , and at 0th step, it was smaller than  $10^{-160}$ . It is known that the gradient vanished through the backward propagation. However, by applying SAL at every step, it increased rapidly, and the error signal reached a value of the same order as the 300th step in the 2nd epoch and then stopped to increase. After around 30 epochs of learning, all 4 error signals are decreased gradually in a similar way as the final error in (1) decreased.

Figure (4) shows the average and standard deviation of sensitivities over all the 20 hidden neurons and all 300 steps during learning. The lower graph in Fig. (4) shows the number of neurons to which SAL was applied even once during the 300 steps. Soon after the learning began, the sensitivity increased and the average value reached 1.0. Then each neuron stopped the SAL, and the value did not change so much keeping the average a bit larger than 1.0. However,

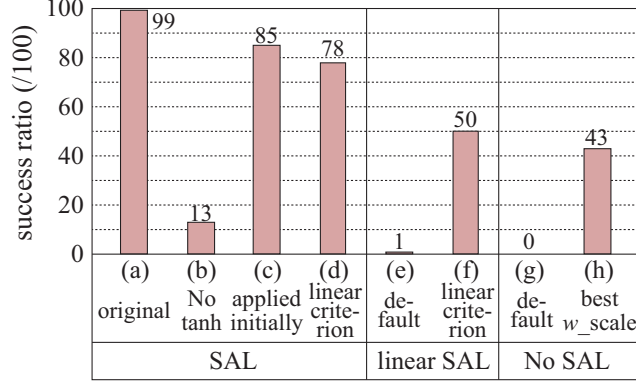


Figure 13: Comparison of success ratio in 100 simulation runs among various conditions in the learning of sequential 3-bit parity problem. In "linear SAL", only linear term (the 1st term as in Eq. (33)) was used in SAL. In "No tanh", tanh was not applied in backward computation. In "linear criterion", only  $|\mathbf{w}|$  was used as sensitivity to decide the application of SAL.

it can be seen that SAL was applied in some neurons afterwards because the sensitivity average for such neurons decreased below 1.0. We can also see that the sudden change in the output in Fig. (2) mentioned above was caused by the SAL application around 30 epoch.

On the other hand, when SAL was not applied and only BPTT was performed, no successful run can be seen as in Fig. 13(g). In RNNs such as a reservoir, the spectral radius of the feedback weight matrix is usually tuned manually to control the network dynamics. Then the spectral radius of  $\mathbf{W}_{FB}$  was increased by 0.01 from 1.0. The maximum success ratio was 43 when the spectral radius is 1.38 as in Fig. 13(h), but it is still far below the case when SAL was applied.

To analyze how the SAL affects the learning positively, 5 other cases are also simulated as shown in Fig. 13. Before entering the analysis of SAL itself, let us see the effect of applying tanh in the backward error computation as expressed in Eq. (38) at first. Fig. 13(b) shows the success ratio when SAL is applied without applying tanh function in error back propagation in BPTT. In the failure cases, gradient or propagated error signals were exploded though SAL was stopped when average sensitivity was larger than 1.0 in each neuron. That could be because of varying sensitivity due to the term  $f'(U)$  in Eq. (3) and/or the delay due to the average presented in Eq.(40). Therefore, to avoid such a gradient explosion, it is a good idea to use tanh also in the backward error computation. In the following, tanh is always applied in the backward computation.

At first, the effect of continuous learning is shown. In the case of Fig. 13(c), SAL was applied only until the sensitivity reaches 1.0 at first. The ratio is worse than the original case. Fig. 14 (B) shows the learning process when the initial weights were the same as (A) but the learning failed. As shown in (3), the propagated error signals reached  $10^{-1}$  order at the second epoch, but soon after that, the error signal at the earlier steps decreased more though the error signal at the 300th step was not decreased. As shown in (4), the sensitivities became more than 1.0 once, but they decreased below 1.0. By comparing with the original case of (A), it is suggested that SAL is useful not only at the beginning of learning, but also works to prevent the loss in sensitivities by BPTT during learning.

Secondly, the effect of nonlinear part  $f'(U)$  of the sensitivity expressed in Eq. (3) is shown. The nonlinear property influences mainly two parts in SAL. One of them is the second term in the second parenthesis in Eq. (33) for weight modification. The other one is that sensitivity including  $f'(U)$  is used as the criteria to decide whether SAL is applied or not. We compare 4 combinations of the two conditions, each of them is linear or nonlinear. In the original case (a) in Fig. 13, both are nonlinear. In (d), SAL itself is nonlinear, but when  $|\mathbf{w}_{FB}|$  is larger than 1.0, SAL was stopped instead of using the sensitivity in Eq. (3) as the criteria for applying SAL. The success ratio is smaller than the original case. Since  $f'(U)$  is smaller than 1.0, the adjustment target value should be larger than 1.0, but it is not so easy to find the optimal value.

Next, from the SAL itself, the nonlinear term that is the second parenthesis in Eq. (33) was removed. When the criterion to stop SAL is nonlinear, as can be seen in Fig. 13(e), learning succeeded only in one simulation run. To investigate this situation, we show a learning process for 60 epochs from the beginning as shown in Fig. 15. The initial weights are the same as the case of Fig. 14. In the case of the original (A), once the sensitivity is larger than 1.0, the weight vector is not larger anymore as can be seen in Fig. (3). The mean absolute value of the output is almost less than 0.5 in Fig. (2). On the other hand, in the case of linear SAL (B), the sensitivities of the two hidden neurons (the

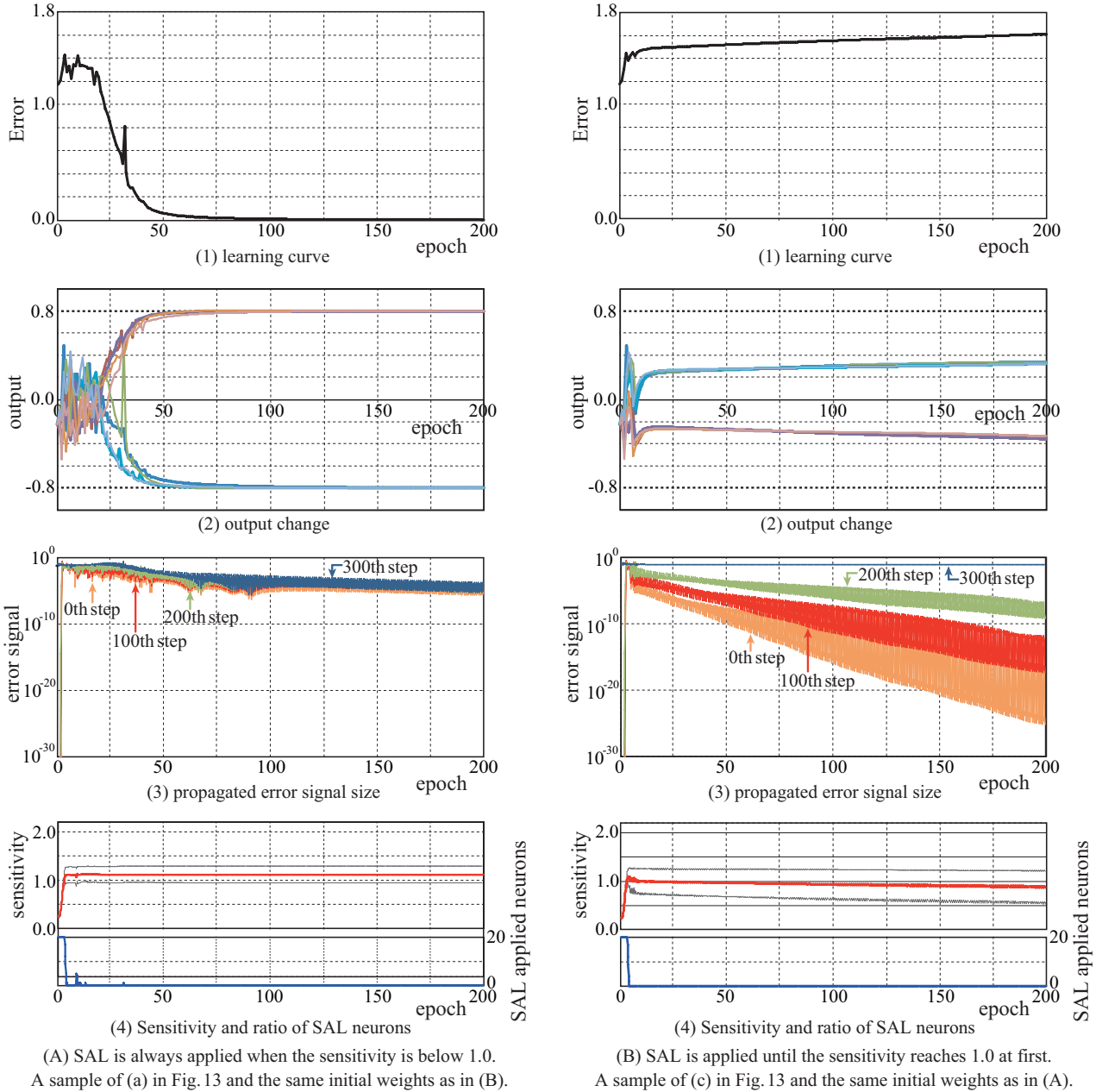


Figure 14: Learning process for sequential 3-bit parity problem with 300 step lag in one example and comparison of two cases (A) and (B) that corresponds to (a) and (c) in Fig. 13 to see the effect of continuous application of SAL during learning. The initial connection weights are the same between (A) and (B). From the top (1) change of RMS error over 4 patterns, (2) change of output for each pattern, (3) RMS of the magnitude of propagated error signal over 10 neurons at several timings in the 1000 steps of backward computation for BPTT. (4) upper: distribution of sensitivity over all the neurons and steps (three lines show the mean (center) and standard deviation) and lower: number of neurons at which SAL is applied at least once in the epoch. (3) and (4) are plotted for the set of forward and backward computations for each pattern presentation. In each line in (3)(4), 4 points are plotted in order of 4 patterns for each epoch. In the 0th epoch, no learning is applied, but the output and sensitivities are observed.



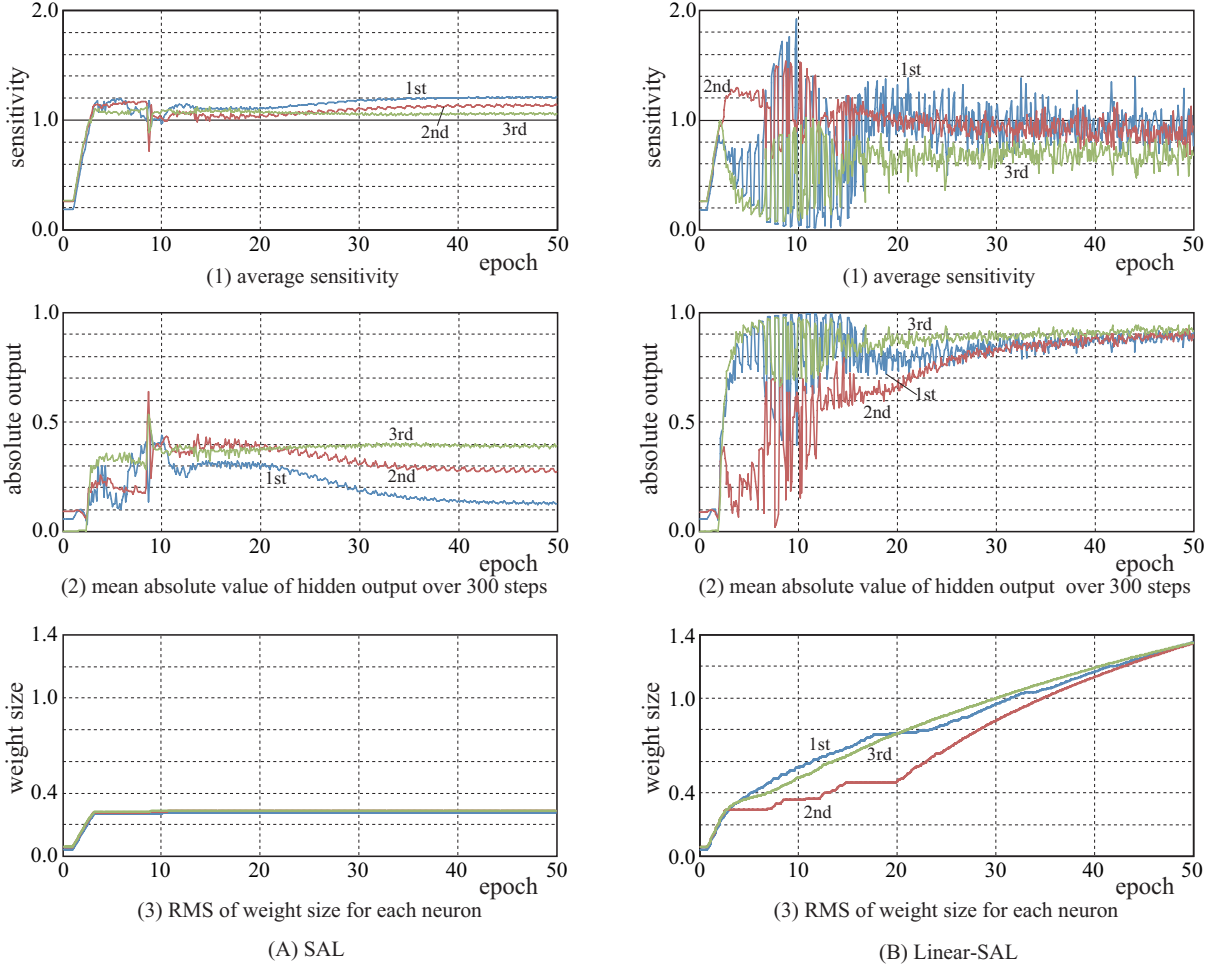


Figure 15: Comparison of the early stage of the learning process (sensitivity  $s$ , absolute output  $|o|$ , weight size  $|w|$  of the first 3 hidden neurons.) for sequential 3-bit parity problem with 1000 step lag by whether the nonlinear term is included (A) or not (B) in SAL. Each of them is an example in the case of Fig. 13 (a) and (d), and the initial weights are the same as in Fig. 14.

first (blue) and third (green) lines) decreased from around 1.0 as in Fig. (1) even though the weight sizes continued to increase as in Fig. (3). We can see that when a sensitivity in (1) decreases, the mean absolute output of the neuron in (2) increases including the large fluctuation depending on the presented pattern. The difference suggests that the nonlinear term in SAL works to prevent the outputs from staying in the saturation area and to keep the sensitivities large.

If the criterion for applying SAL is also linear (see Fig. (f)), learning succeeded in half of the runs. In this case, since the linear criteria is larger as the weight vector increases, linear SAL stopped and the weights do not increase to very large values. The success ratio is slightly larger than the best ratio when the scale of the weight matrix is manually explored in Fig. 13(h). That must show the positive influence of nonlinear SAL.

#### 4.2.2 Case of deep feedforward neural network (DFNN)

Finally, we applied sensitivity adjustment learning (SAL) to a DFNN. In order to see the effect of number of layers clearly, we employ an 8-bit parity problem with noise addition as a simple nonlinear problem. There are 8 inputs, each of them takes a value of -1 or 1. There is only one output, and if the number of 1 values in the inputs is odd, the ideal value is 0.8, and -0.8 otherwise. The number of patterns is  $2^8 = 256$ . There are some hidden layers, and each of which has 20 neurons. Here, also to show the effectiveness of SAL clearly, simple stochastic gradient descent (SGD) method is used, and learning is not applied to a batch or mini-batch, but applied for each pattern presentation.

Table 4: Parameters for supervised learning of DFNNs using SAL and BP.

parameter		value
initial connection weights (uniformly random)	input $\rightarrow$ hidden	$[-0.1, 0.1]$
	hidden $\rightarrow$ output	$[-0.1, 0.1]$
	hidden $\rightarrow$ hidden	varied or $[-0.1, 0.1]$
learning rate $\eta_{BP}$ in Eq. (36)	input $\rightarrow$ hidden	0.02
learning rate $\eta_{SAL}$ in Eq. (33)		0.002
decay rate $\beta$ in Eq. (40)		0.999
num of neurons in each hidden layer		20
magnitude of noise vector for input		0.2
learning epochs		5,000

Table 5: Learning rate  $\eta_{BP}$  except for the weights from the inputs to the hidden neurons.

num of layers	3	5	10	30
learning rate	0.01	0.003	0.001	0.0007
num of layers	100	200	300	1000
learning rate	0.0005	0.0004	0.0003	0.0001

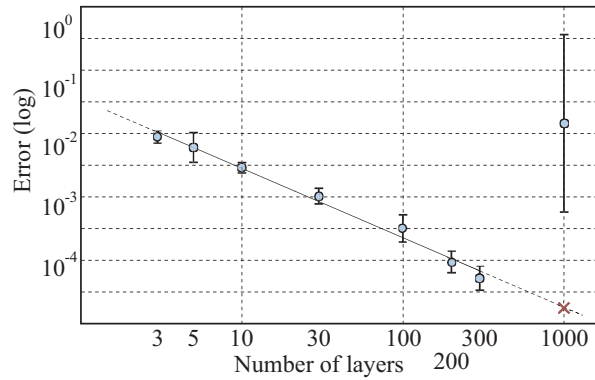


Figure 16: The relation between the number of layers and average error in log-scale for 8-bit parity problem with noise addition. The average and standard deviation over 20 simulation runs with different initial weights are shown for each plot. The x mark at the 1000 layer shows the error when learning succeeded only once. That was the least error for all the  $20 \times 8$  runs. The line indicates the linear approximation from 3 layers to 300 layers.

The used parameters are presented in Table 4. Except for the lowest hidden layer that receives inputs, the learning rate  $\eta_{BP}$  for SGD is the same for all the layers, but different depending on the number of layers as shown in Table 5. Initial connection weights are decided randomly in a range of  $[-init\_W, init\_W]$ . Here,  $init\_W$  is called the initial weight scale that is the same for all the hidden layers.

At first, learning performance is observed as the number of layers varies from 3 to 1000. Figure 16 shows the mean and standard deviation of log-scaled RMS error over 256 patterns after learning in 20 simulation runs with a different random sequence for initial weights and noises. The NN can learn the problem even with 300 hidden layers without employing special architectures. We observe that the performance improves as the number of layers increases, and the errors lay almost on the line of linear approximation in the log-scale. In the case of 1000 layers, learning succeeded only once. The error for the run lays on the line of linear approximation until 300 layers, and was the best of all the  $20 \times 8$  runs.

Next, learning performances with various initial connection weight scales are observed. Fig. 17(a) shows results when SAL was not applied, and Fig. 17(b) shows the result when SAL was applied. The performances are plotted for 4 cases varying the number of layers as 30, 100, 200, 300, and each plot is the average over 20 simulation runs with different random sequences.

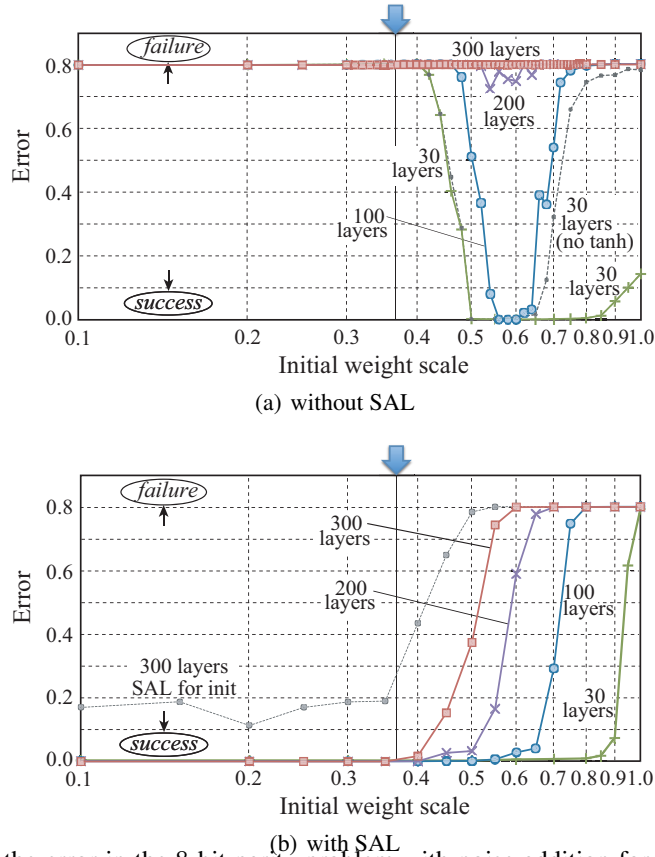


Figure 17: Comparison of the error in the 8-bit parity problem with noise addition for various initial weight scales between the cases of (a) only BP (back propagation) and (b) SAL (sensitivity adjustment learning)+BP. The number of layers is varied in 30, 100, 200, 300. The average of the RMS error after learning over 20 simulation runs is shown for each plot. In (a), the case in which tanh is not applied in BP is also shown for the case of 30 layers. In (b), the case in which SAL is applied only until the sensitivity reaches 1.0 at first is also shown for the case of 300 layers.. The vertical line and the arrow between 0.3 and 0.4 in the horizontal axis indicates the value with which the spectral radius of the weight matrix is expected to be 1.0

In the case of (a) ‘without SAL’, when the initial weight scale is less than 0.4, learning failed even in the case of 30 layers. The learning performance seems the best around the initial weight scale is 0.5 or 0.6 where the expected spectral radius (maximum absolute eigenvalue) of the weight matrix is around 1.5, and the error is lower as the number of layers is smaller. When the weight scale becomes larger than the optimal scale, the error increases again. Those can be due to the influence of the vanishing/exploding gradient. However, when the number of layers is 300, even though the step size of varying the initial weight scale is as small as 0.01, there is no scale with which the error becomes smaller than around 0.8.

The result when the SAL is applied with BP is shown in Fig. 17(b). When the initial weight scale was large, learning failed. However, we can see that if the initial weight scale is set to a small value like 0.1, learning succeeded in all the 20 simulation runs regardless of the numbers of layers. The boundary scale between learning success and failure is smaller as the number of layers becomes larger. From Fig. 16 where the vertical axis is log-scaled, when the scale is 0.1, the error becomes smaller as the number of layers is higher. That is the opposite trend of the case of ‘without SAL’.

Figure 18 shows the RMS of the propagated error signal  $\delta$  over all the 20 neurons at the bottom hidden layer in the first epoch when SAL or BP did not update the weights. At the arrow around the weight scale 0.37, the average spectral radius of the weight matrices from the bottom to the top hidden layers is expected to be 1.0. However, by the effect of nonlinear activation function, the error signal actually became large when the scale is around 0.58 or 0.6. The weight scale is almost the same as when the performance is best in Fig. 17(a). This suggests the vanishing/exploding gradient was the cause of the bad learning performance when SAL was not applied.

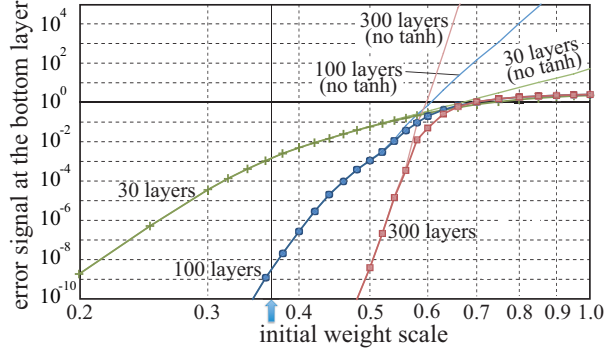


Figure 18: Propagated error signal  $\delta$  at the bottom hidden layer before learning.

On the other hand, even though the error signal reaches the bottom layer, there is no weight scale with a smaller error when the number of layers is 300. In the case of 200 layers, the error becomes slightly small around 0.58 initial weight scale, but the error was considerably smaller when SAL was applied with a small initial weight scale. This means that only adjusting the initial weight scale is not enough to learn appropriately.

We consider two reasons for the good performance when SAL was applied. The error when SAL is only applied at the beginning of learning is additionally plotted in Fig. 17(b) for the case of 300 layers. The learning sometimes failed as well as the case of RNN in Fig. 13 (c). This means that sensitivity should be moderate not only at the beginning of learning, but also during learning. However, in this case, although it occasionally failed to learn but in many other cases, the error was equivalent to the case when SAL is always applied. The second reason can be that by adjusting the initial weight scale only, the maximum eigenvalue can be moderate, but the sensitivities are not moderate for all the neurons especially when the number of inputs is small. SAL makes it moderate for all the neurons through learning. Actually, it was confirmed that the Euclidean norm of each weight vector  $|\mathbf{w}|$  was adjusted around 1.1 in each neuron, sometimes learning succeeded even without applying SAL when the number of layers is 300.

Finally, processing through many layers is observed. After learning, we set continuous uniform random numbers ranges from -1.0 to 1.0 as the input of the network. 100 sets of inputs are given to each of the 20 networks after learning, and all the 2,000 data were observed. Figure 19 shows the histogram of the outputs when the number of layers is set to 3, 10, 30, 100, 300. As the number of layers increase, the frequency around -0.8 or 0.8 becomes larger. Attractor-like processing through layer can be seen when the number of layers is large, bringing out the high learning performance as presented in Fig. 16.

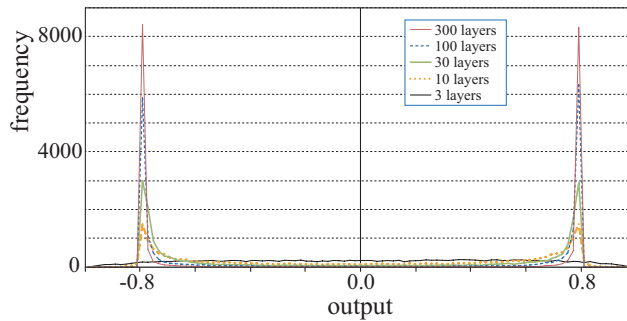


Figure 19: Histogram of the network output when 1000 continuous random inputs each of them is decided randomly from -1.0 to 1.0 is put into 20 networks after learning. The effect of the number of layers is compared.

Then the transition of the hidden representation is observed when the number of layers is 300. Figure 20 shows the hidden outputs for the random 1000 continuous inputs after PCA (principle component analysis) in each of the first (lowest), 100th, 199th, 298th (highest) hidden layers. Among 20 simulation runs, we pick up one whose transition of representation can be seen easily. We can see the representation is extended and fold gradually like the baker's transformation, and the internal states are divided into two lumps finally.

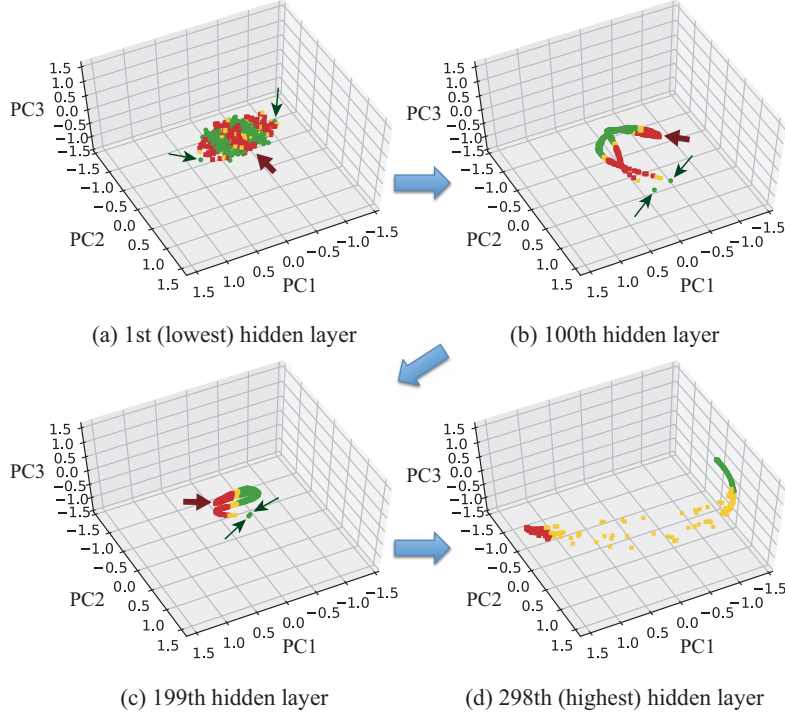


Figure 20: Change of internal representation after PCA through layers for 1000 continuous random inputs after learning. (One sample of 20 networks in Fig. 19) The plot color and shape indicate the final network output as ‘□’(red):  $0.75 < o < 0.85$ , ‘○’(green):  $-0.85 < o < -0.75$ , ‘×’(gold): others. Each of the 3 arrows shows how a specific point or group of points moves through layers.

## 5 Discussion & Conclusion

We believe that in the future, higher functions such as conversation and thinking will be desired and so the control of dynamics in recurrent neural networks (RNNs) will be more and more critical. Towards such a future, we have shown the possibility that only by controlling the sensitivity in each neuron, the global dynamics of RNNs can be controlled. When the sensitivity adjustment learning (SAL) is applied to an RNN, the log sensitivity is almost identical to the maximum Lyapunov exponent before the network dynamics get into chaos not depending on the number of neurons, connection ratio or number of layers. In particular, when the sensitivity of each neuron is adjusted to 1.0 by SAL, the maximum Lyapunov exponent of the entire network becomes 0.0. That means the dynamical state of ‘edge of chaos’, which is very important from information processing perspective, is achieved autonomously through SAL by merely setting the target sensitivity to 1.0 in each neuron in an RNN.

We have also shown that SAL with 1.0 target sensitivity leads to avoiding ‘vanishing gradient’ in gradient-based learning simultaneously in RNNs, and that is also valid in deep feedforward neural networks (DFNNs). The combination of SAL and BP or BPTT enables to solve the problems without introducing special architecture or computation except for general local learning from small initial weights, and the performance is better than when the initial weight scale is finely tuned without applying SAL. When the values of the weights are small, SAL simply increases the magnitude of each weight vector without changing the vector direction, and so it seems to be equivalent to just increasing the weights gradually at a glance. However, we could see the advantage of locality, continuity and nonlinearity from the above learning results as follows.

- The computation is entirely local and also the decision to stop the SAL can be made autonomously by each neuron itself. The spectral radius or eigenvalues of a weight matrix cannot be computed locally in each neuron.
- In the sensitivity, not only linear transformation by the weight vector, but also the nonlinear transformation by the activation function can be considered. Therefore, the criterion to stop the SAL can be just 1.0, which corresponds to the edge of chaos when the network is an RNN. It is not easy to decide the appropriate spectral radius easily, because the influence of nonlinear transformation is varied.

- Nonlinear term in SAL prevents the output from staying in the saturation area of the activation function, and good information transmission is maintained in both forward (output) and backward (error) computation.
- By applying SAL with another learning simultaneously, SAL can prevent the decrease of sensitivity caused by the other learning.
- Sensitivities are not adjusted for each layer, but more finely for each neuron.

These mean that we are no longer free from the fine tuning of the initial weight scale, and furthermore the learning performance is better.

When network dynamics is around the ‘edge of chaos’, activities for learning is generally high[11]. In such dynamics, a small perturbation in the forward computation or the propagated error signal in the backward computation can be maintained as mentioned earlier. In the chaos-based reinforcement learning we proposed, internal chaotic dynamics are the origin of ‘exploration’ of the agent. On the other hand, learning generally forms attractors to increase reproducibility for better states or actions, and makes the state transition from irregular to rational. That enables autonomous transitions from ‘exploration’ or ‘wandering’ to ‘exploitation’ or ‘thinking’ through learning.

However, it sometime leads to a loss of sensitivity. If the network dynamics turns into non-chaotic, the network cannot keep an active state for learning, and in the worst case, the agent cannot explore or learn any more. This means ‘death’ for the agent. In our previous works, an autonomous resume of exploration in unknown environments could be seen without learning except for reinforcement learning[18][11]. However, naive parameter tuning is required. Therefore, it is significant that SAL guarantees to maintain moderate sensitivities, which lead to agent’s activities. We also expect that when SAL is applied in a high dimensional space, formed attractors through learning are not complete but strange by keeping the sensitivities around 1.0, and such behaviors as chaotic itinerancy can be seen. We expect that leads to the emergence of ‘inspiration’ or ‘discovery’, although it should be investigated in more detail.

In reservoirs that have yielded outstanding results in time series data processing and temporal pattern generation, appropriate scale of random weight values is essential. However, the proposed method can also be an answer to the question of how each neuron gets such moderate weights autonomously. Nevertheless, the existence of small random weights is still assumed before applying SAL. For being more plausible, we aim to examine the situation in which the initial weights are decided considering the physical distance to downstream neurons and so on without using random numbers.

We believe SAL is significant also in terms of autonomous decentralized processing that enables to control the global dynamics of the network by local learning of each neuron. In the current neural network computation, parallel processing is often utilized by using GPUs, but they are still under the control of a centralized system. Yet in the future, if the network becomes larger and more flexible like our brain and is trained and utilized in real time, parallelization at the level of each neuron and autonomous decentralized processing will be essential[29]. The proposed method in this paper lies in this direction, and we also expect to accelerate researches in this direction.

Other future directions of this research are discussed as follow. The current study focused on the analysis of SAL behavior, and we employed simple learning problems when examining the combination of SAL and BP. Therefore, it is strongly expected to apply SAL to more practical and large-scale complicated problems and compare the performance with the other methods. Some problems still remain in our study. For example, naive learning rate adjustment is still necessary while we no longer need to care about the initial weight scale. Another possible future research can investigate cases where SAL increases the error for the other learning like the case in Fig. 14(b).

Another important unsolved problem is to examine whether SAL works when a neuron receives both feedback and external inputs in an RNN. In this paper, SAL was applied mainly to the connection weights between hidden layers including feedback connections. In reinforcement learning problems, the feedback loop through the outer world from actions to perceptions for an agent also influences the network dynamics. In this paper, in two-layer networks, the global network dynamics could be controlled by SAL not depending on the network architecture. In this case, for one of the two layers, the other layer can be considered as a part of the outer world. Accordingly, we hope SAL works without discriminating external and internal inputs. We also want to examine whether SAL works in dynamical neurons (continuous-time model) that enables variable time constant or chaotic neurons with refractoriness.

We are living not only in space, but also in time. However, most of the existing learning methods have focused on the state or output at a time, which can be expressed as a point in space and move it to be better by learning. Even though an RNN is used and the state or output changes along time, learning has not considered the flow of the state or output, which is expressed as a line in space. The sensitivity is the index for the flow or dynamics in the processing of one neuron. We hope the sensitivity is the key to develop learning methods to control the flow. What is the most desirable investigation at the moment is to bring this idea “learning of flow” into reinforcement learning and establish a new paradigm of dynamic reinforcement learning, where the output or state at a specific timing is not learned directly but

the dynamics are learned directly from the viewpoint of ‘exploration’ or ‘reproducibility’ in high-dimensional systems, as a fundamental technology towards the emergence of ‘thinking’.

## Acknowledgment

We would like to thank Prof. Hiromichi Suetani for useful suggestions about chaotic dynamics. We also thank our laboratory members for discussions and sharing related simulation results. This work was supported by JSPS KAKENHI Grant Number JP15K00360, JP20K11993 and also Kayamori Foundation of Informational Science Advancement K31-KEN-XXIV-539.

## References

- [1] L. Jiao, F. Zhang, F. Liu, S. Yang, L. Li, Z. Feng, R. Qu, A survey of deep learning-based object detection [abs/1907.09408](https://arxiv.org/abs/1907.09408). [arXiv:1907.09408](https://arxiv.org/abs/1907.09408).  
URL <http://arxiv.org/abs/1907.09408>
- [2] A. Nassif, I. Shahin, I. Attili, M. Azzeh, K. Shaalan, Speech recognition using deep neural networks: A systematic review, *IEEE Access* PP (2019) 1–1.
- [3] H. I. Fawaz, G. Forestier, J. Weber, L. Idoumghar, P. Muller, Deep learning for time series classification: a review [abs/1809.04356](https://arxiv.org/abs/1809.04356). [arXiv:1809.04356](https://arxiv.org/abs/1809.04356).  
URL <http://arxiv.org/abs/1809.04356>
- [4] D. W. Otter, J. R. Medina, J. K. Kalita, A survey of the usages of deep learning in natural language processing [abs/1807.10854](https://arxiv.org/abs/1807.10854). [arXiv:1807.10854](https://arxiv.org/abs/1807.10854).  
URL <http://arxiv.org/abs/1807.10854>
- [5] Y. Bengio, P. Simard, P. Frasconi, Learning long-term dependencies with gradient descent is difficult, *IEEE Transactions on Neural Networks* 5 (2) (1994) 157–166.
- [6] S. Hochreiter, The vanishing gradient problem during learning recurrent neural nets and problem solutions, *Int. J. Uncertain. Fuzziness Knowledge-Based System* 6 (2) (1998) 107–116.
- [7] R. Pascanu, T. Mikolov, Y. Bengio, On the difficulty of training recurrent neural networks, in: *Proceedings of the 30th International Conference on International Conference on Machine Learning - Volume 28, ICML'13, JMLR.org*, 2013, pp. III–1310–III–1318.
- [8] I. B. Yildiz, H. Jaeger, S. J. Kiebel, Re-visiting the echo state property, *Neural networks : the official journal of the International Neural Network Society* 35 (2012) 1–9.
- [9] D. C. Sussillo, Learning in chaotic recurrent neural networks, Ph.D. thesis, USA, aAI3346497 (2009).
- [10] T. Matsuki, K. Shibata, Reward-based learning of a memory-required task based on the internal dynamics of a chaotic neural network, in: A. Hirose, S. Ozawa, K. Doya, K. Ikeda, M. Lee, D. Liu (Eds.), *Neural Information Processing. ICONIP 2016. Lecture Notes in Computer Science*, Vol. 9947, Springer International Publishing, 2016, pp. 376–383.
- [11] T. Matsuki, K. Shibata, Adaptive balancing of exploration and exploitation around the edge of chaos in internal-chaos-based learning, *Neural Networks* 132 (2020) 19–29.
- [12] K. Shibata, Functions that emerge through end-to-end reinforcement learning – the direction for artificial general intelligence –, in: [arXiv:1703.02239v2](https://arxiv.org/abs/1703.02239v2), *The 3rd Multidisciplinary Conf. on Reinforcement Learning and Decision Making (RLDM)17*, 2017.
- [13] Y. Sawatsubashi, M. F. bin Samsudin, K. Shibata, Emergence of discrete and abstract state representation through reinforcement learning in a continuous input task, in: *Advances in Intelligent Systems and Computing, Robot Intelligence Technology and Applications 2012*, 2012, pp. 13–22.
- [14] K. Shibata, M. Sugisaka, Dynamics of a recurrent neural network acquired through learning a context-based attention task, *Artificial Life Robotics* 7 (2004) 145–150.
- [15] H. Utsunomiya, K. Shibata, Contextual behavior and internal representations acquired by reinforcement learning with a recurrent neural network in a continuous state and action space task, in: *Advances in Neuro-Information Processing, Lecture Note in Computer Science*, Vol. 9, 2009, pp. 970–978.
- [16] K. Shibata, H. Utsunomiya, Discovery of pattern meaning from delayed rewards by reinforcement learning with a recurrent neural network, in: *Proc. of IJCNN 2011*, 2011, pp. 1445–1452.

- [17] K. Shibata, K. Goto, Emergence of flexible prediction-based discrete decision making and continuous motion generation through actor-q-learning, in: Proc. of ICDL-Epirob 2013, 2013, p. ID 15.
- [18] K. Shibata, Y. Sakashita, Reinforcement learning with internal-dynamics-based exploration using a chaotic neural network (2015) #15231.
- [19] K. Shibata, Y. Goto, New reinforcement learning using a chaotic neural network for emergence of "thinking" - "exploration" grows into "thinking" through learning - abs/1705.05551. arXiv:1705.05551.  
URL <http://arxiv.org/abs/1705.05551>
- [20] Y. Goto, K. Shibata, Influence of the chaotic property on reinforcement learning using a chaotic neural network, in: D. Liu, S. Xie, Y. Li, D. Zhao, E. El-Alfy (Eds.), Neural Information Processing. ICONIP 2017. Lecture Notes in Computer Science, Vol. 10634, Springer International Publishing, 2017, pp. 759–767.
- [21] K. Sato, Y. Goto, K. Shibata, Chaos-based reinforcement learning when introducing refractoriness in each neuron, in: In: Kim JH., Myung H., Lee SM. (eds) Robot Intelligence Technology and Applications. RiTA 2018. Communications in Computer and Information Science, 2012, pp. 13–22.
- [22] S. Hochreiter, J. Schmidhuber, Long short-term memory, *Neural Comput.* 9 (8) (1997) 1735–1780.
- [23] J. Chung, Ç. Gülçehre, K. Cho, Y. Bengio, Empirical evaluation of gated recurrent neural networks on sequence modeling, CoRR abs/1412.3555.  
URL <http://arxiv.org/abs/1412.3555>
- [24] K. He, X. Zhang, S. Ren, J. Sun, Deep residual learning for image recognition.  
URL <http://arxiv.org/abs/1512.03385>
- [25] S. Ioffe, C. Szegedy, Batch normalization: Accelerating deep network training by reducing internal covariate shift, in: Proceedings of the 32Nd International Conference on International Conference on Machine Learning - Volume 37, ICML'15, JMLR.org, 2015, pp. 448–456.
- [26] J. L. Ba, J. R. Kiros, G. E. Hinton, Layer normalization.  
URL <https://arxiv.org/abs/1607.06450>
- [27] T. Salimans, D. P. Kingma, Weight normalization: A simple reparameterization to accelerate training of deep neural networks, in: D. D. Lee, M. Sugiyama, U. V. Luxburg, I. Guyon, R. Garnett (Eds.), Advances in Neural Information Processing Systems 29, Curran Associates, Inc., 2016, pp. 901–909.
- [28] G. Klambauer, T. Unterthiner, A. Mayr, S. Hochreiter, Self-normalizing neural networks, in: In Advances in Neural Information Processing Systems 30 (NIPS), 2017.
- [29] Y. Okabe, T. Kouhara, H. Hayashi, A. Narusawa, M. Kitagawa, K. Miyao, Moderatism: New concept for self-organization of neural networks, in: Proc. of 2nd Int'l Conf. on Knowledge-based Intelligent Electronic Systems, 1998, pp. 246–249.
- [30] E. Ott, C. Grebogi, J. A. Yorke, Controlling chaos, *Physical Review Letter* 64 (1990) 1196–1199.
- [31] I. Ighneiwa, S. Hamidatoua, F. B. Ismaela, Using artificial neural networks (ANN) to control chaos, CoRR abs/1701.00754.  
URL <http://arxiv.org/abs/1701.00754>
- [32] C. G. Langton, Computation at the edge of chaos: phase transitions and emergent computation, *Physical D: Nonlinear Phenomena* 42 (1990) 12–37.
- [33] R. Legenstein, W. M. S. M. Chase, A. B. Schwartz, A reward- modulated hebbian learning rule can explain experimentally observed network reorganization in a brain control task, *J. of Neuroscience* 30 (2010) 8400–9410.
- [34] J. Boedecker, O. Obst, J. T. Lizier, N. M. Mayer, M. Asada, Information processing in echo state networks at the edge of chaos, *J. of Neuroscience* 30 (2010) 8400–9410.
- [35] C. A. Skarda, W. J. Freeman, How brains make chaos in order to make sense of the world, *Behavioral and brain sciences* 10 (1987) 161–173.
- [36] W. J. Freeman, The physiology of perception (February 1991).
- [37] Y. Osana, M. Hagiwara, Successive learning in hetero- associative memory using chaotic neural networks, *Int'l Journal of Neural Systems* 9 (1999) 285–299.